Imaging Agents

Water-Soluble Photoluminescent Silicon Quantum Dots**

*Jamie H. Warner, Akiyoshi Hoshino, Kenji Yamamoto, and Richard. D. Tilley**

The quantum confinement of excitons in semiconductor quantum dots leads to interesting optical properties that can be exploited in a range of photonic applications including biological fluorescence imaging[1–6] and optoelectronic devices.[7–13] Quantum dots are becoming popular as replacements for fluorescent dyes in biological fluorescence imaging because of their superior stability against photobleaching. To date, considerable emphasis has been placed on using CdSe quantum dots with a ZnS shell as biological chromophores since they emit light that can be tuned throughout the visible spectrum.[14] However, concerns have been raised about the toxicological issue of using cadmium in biological systems.[15] In particular, Derfus et al. showed that CdSe quantum dots without a ZnS shell were toxic to liver cells after exposure to UV light.[15] The potential biocompatibility of silicon makes photoluminescent silicon quantum dots an ideal candidate for biological fluorescence imaging and should eliminate any potential toxicology problems that might arise from having a CdSe core.[16,17]

Strong quantum confinement in silicon increases the probability of radiative recombination through the direct band gap transitions and reduces phonon-assisted indirect band gap transitions.[18] In silicon, this requires the physical dimensions of the quantum dots to be on the order of or less than the bulk exciton Bohr radius of 4 nm.[19,20] Quantum dot sizes of less than 8 nm are easily achieved using wet chemistry techniques.[19–22] The remarkably successful advances in the synthesis of the semiconductor groups II/VI and III/V have not been applied to silicon as a consequence of the relatively high temperatures required to degrade the precursor and to produce highly crystalline quantum dots. The greatest success in producing silicon quantum dots with strong quantum confinement to date has been by the solution-phase reduction of silicon salts.[19,21,22]

[*] J. H. Warner, R. D. Tilley
School of Chemical and Physical Sciences
MacDiarmid Institute of Advanced Materials and Nanotechnology
Victoria University of Wellington
P.O. Box 600, Wellington (New Zealand)
Fax: (+64) 4-463-5237
E-mail: richard.tilley@vuw.ac.nz
A. Hoshino, K. Yamamoto
Department of Medical Ecology and Informatics
Research Institute
International Medical Center of Japan
Toyama 1-21-1, Shinjuku, Tokyo 162-8655 (Japan)

[**] J.W. and R.D.T. thank the MacDiarmid Institute of Advanced Materials and Nanotechnology for funding. J.W. and R.D.T. thank H. Rubinsztein-Dunlop for the use of the time-resolved PL spectroscopy system at The University of Queensland.

The solution-phase synthesis of silicon quantum dots has previously been reported by Kauzlarich and co-workers[21,22] through the use of a variety of reducing agents, by Korgel and co-workers[19,23] through the use of high temperatures and pressures, and by Wilcoxon et al. by using micelles.[20,24] The current problem associated with the simpler room-temperature syntheses [20–22] is the large size distribution produced. The large size distribution prevents a simple interpretation of the optical spectra. Post-synthesis treatments for narrowing the size distribution of the silicon quantum dots, such as high-pressure gas chromatography (HPGC), have revealed sharp features in the absorption spectra and narrow photoluminescence spectra attributed to direct band gap transitions.[20] We have recently reported the synthesis of 1–2-nm silicon quantum dots that were surface-passivated by 1-heptene. These dots had a narrower size distribution than previously reported and gave a strong blue photoluminescence.[25]

For silicon quantum dots to be used in biomedical applications it is essential that they have a substantial photoluminescence quantum yield in the visible region, have a fast radiative recombination rate, and are water soluble and hydrophilic to prevent aggregation and precipitation in a biological environment. The chemical process used to terminate the surfaces of the silicon quantum dots changes the internal electronic structure and thus plays an important role in the resultant emission wavelength and radiative lifetime, and ultimately determines the solubility.[18] Silicon quantum dots with an oxide surface passivation typically display a dipole-forbidden yellow-red emission with radiative lifetimes of 10^{-3}–10^{-6} s.[18,26] This slow rate of recombination limits the use of oxide-passivated silicon quantum dots in biological imaging. However, silicon quantum dots with a hydrogen or carbon surface passivation have electric-dipole-allowed direct band gap transitions that lead to blue photoluminescence with fast recombination rates of 10^{-8}–10^{-9} s.[18,20]

In this study we describe a simple room-temperature synthesis for producing water-soluble silicon quantum dots that exhibit strong blue photoluminescence with a rapid rate of recombination. The use of hydride reducing agents in these experiments produce hydrogen-terminated particle surfaces.[20,24,25] The Si–H surface bond can then be treated with both a compound containing a C=C bond and a platinum catalyst to produce a variety of surface types through formation of a Si–C surface bond. The surface of the silicon quantum dots are modified with allylamine to form hydrophilic silicon quantum dots (Figure 1). Previous reports of changing the surface-capping molecules of silicon particles have involved treating chloride-terminated particle surfaces with Grignard reagents to produce particles capped with organic molecules[27] or utilized a Si–OR bond.[22] Silicon quantum dots with a chlorine-terminated surface are restricted to a small range of available Grignard reagents, whilst Si–OR bonds have been shown to greatly affect the electronic charge distribution in the silicon quantum dots and consequently reduce the energy of indirect transitions.[18,26]

Figure 2 shows a high-resolution transmission electron microscope (HRTEM) image of a number of allylamine-capped silicon quantum dots on a carbon-coated copper grid.

  DOI: 10.1002/anie.200501256

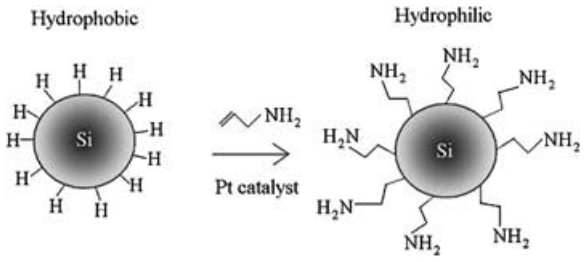

Figure 1. Schematic diagram of the procedure used to change the surface chemistry of the silicon quantum dots from hydrogen to allylamine.

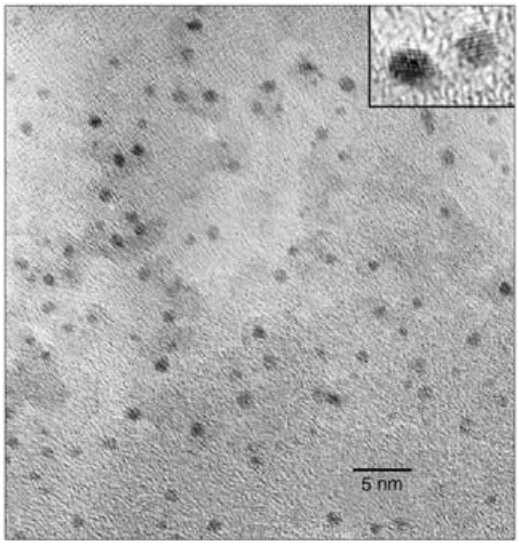

Figure 2. High-resolution transmission electron microscopy (HRTEM) image of a large number of allylamine-capped silicon quantum dots. Inset: HRTEM image of two silicon quantum dots showing the crystal lattice planes.

The water-soluble silicon quantum dots were highly crystalline and the atomic lattice planes of two separate silicon quantum dots can be clearly seen in the inset of Figure 2. Fast Fourier transform (FFT) analysis of the crystal structure shown in the inset of Figure 2 could be matched with the (2,1,−1) and (2,−1,1) planes of diamond silicon when viewed down the [011] direction. The low atomic weight of silicon relative to other metallic and semiconductor quantum dots combined with their extremely small dimensions resulted in low contrast in the HRTEM images. Only by removing almost all of the surfactant (TOAB) could such small (1–2 nm) silicon quantum dots be imaged by HRTEM. Figure 2 shows a relatively high contrast HRTEM image of the 1–2-nm silicon quantum dots along with minimal surfactant, thus indicating that a high level of purification had been achieved. The high purity of the silicon quantum dots enables the photoluminescence to be assigned to the quantum dots and not to other by-products of the reaction, such as silicon-based organosilane polymer/oligomers.

The small dimensions of the silicon quantum dots limits the selected-area electron-diffraction and X-ray diffraction measurements, and no conclusive results have as yet been obtained by using these techniques. The silicon quantum dots were also faceted, which reflects the controlled growth environment.[19] A mean size and size distribution of 1.4 ± 0.3 nm of the allylamine-capped silicon quantum dots was obtained by analyzing 648 quantum dots from different regions on the TEM grid. This small size distribution is a significant improvement on previous reports of 1–2-nm silicon quantum dots synthesized in inverse micelles.[20–22] Energy-dispersive X-ray spectroscopy (EDS) performed on the quantum dots showed a strong peak associated with silicon and no peaks for platinum. This observation confirmed that the platinum catalyst had successfully been removed during purification.

The bonding of allylamine to the surface of the silicon quantum dots was confirmed by FTIR spectroscopy (Figure 3). Peaks were observed at 1460 and 1260 cm^{-1} and

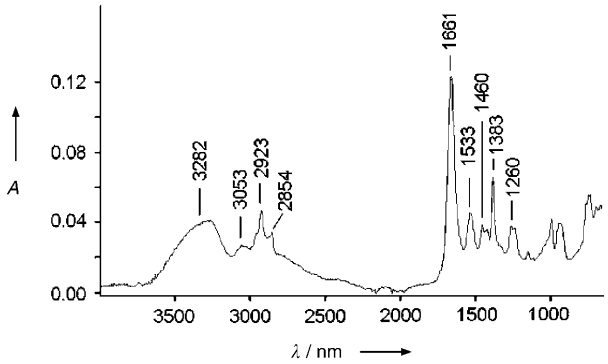

Figure 3. FTIR spectrum of allylamine-capped silicon quantum dots.

attributed to the vibrational scissoring and symmetric bending of $Si{-}CH_2$.[27] The absorbance between 2500 and 3500 cm^{-1} is attributed to symmetric and asymmetric vibrations of the $C{-}CH_2$ and $C{-}NH_3$ molecular components of the allylamine, while the dominant peak at 1661 cm^{-1} is attributed to the allylamine and clearly indicates its attachment to the silicon quantum dots. The peaks between 1000 and 1100 cm^{-1} are attributed to the vibrational stretching of Si–OR.[21] Despite the fact that the silicon quantum dots were heated in atmospheric conditions to remove the solvent for FTIR measurements, the magnitude of the Si–OR vibration is very small when compared to the FTIR reports of siloxane-coated silicon quantum dots, which have a total Si–OR surface coverage.[21] This difference highlights the strength and stability of the Si–C bond formed between the silicon quantum dots and the allylamine as well as the minimal number of Si–OR surface bonds present.

The absorption spectrum of the allylamine-capped silicon quantum dots in water (Figure 4a, curve I) displays a feature at 320 nm which is attributed to the Γ-Γ direct band gap transition.[19,20] This direct band gap transition has blue-shifted because of the effect of quantum confinement in the quantum dots—from the bulk value of 3.4 to 3.8 eV in these silicon quantum dots—and is in good agreement with other reports.[19,20]

The photoluminescence (PL) spectra recorded at 300 and 400 nm (Figures 4a, curves II and III) show a peak at 480 nm

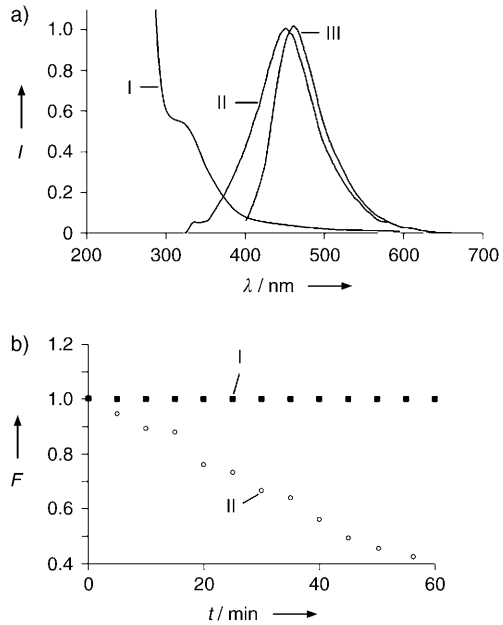

Figure 4. a) Curve I: Absorption spectrum of allylamine-capped silicon quantum dots in water; curve II: photoluminescence spectrum of allylamine-capped silicon quantum dots in water with excitation at 300 nm; curve III: photoluminescence spectrum of allylamine-capped silicon quantum dots in water with excitation at 400 nm. b) Integrated photoluminescence as a function of time of allylamine-capped silicon quantum dots in water (curve I) and rhodamine 6G in water (curve II). An excitation wavelength of 400 nm was used in both cases.

with a full-width at half maximum height (FWHM) of 70–80 nm. All the spectra in Figure 4 have been scaled for clarity of presentation.

Photoluminescence quantum yields of the allylamine-capped silicon quantum dots in water were obtained by using the comparative method of Williams et al.[28] PL quantum yields of up to 10% were obtained relative to the standard, 9,10-diphenylanthracene, in cyclohexane.[29] The optical properties of the colloidal solutions of the allylamine-capped silicon quantum dots were stable for several months. The silicon quantum dots showed better photobleaching stability than the fluorescent dye, rhodamine 6G in water, on excitation with UV light (Figure 4b). The silicon quantum dots showed no signs of any measurable photobleaching (Figure 4b, curve I) under the same illumination conditions during which the photoluminescence from rhodamine 6G dropped by 60% (Figure 4b, curve II).

The origin of the photoluminescence observed in Figure 4 is complicated by the combination of both indirect and direct band gap transitions present in silicon quantum dots and is actively debated.[19] However, there is strong theoretical evidence suggesting that 1–2-nm silicon quantum dots with a hydrogen or carbon surface termination have direct band gap optical transitions that lead to photoluminescence in the UV/blue region of the electronic spectrum.[18] The emission observed in Figure 4a is consistent with the theoretical predictions of direct band gap recombination in silicon quantum dots with carbon surface termination rather than from trap states or surface states, or of silicon quantum dots with oxygen surface termination. Emission from a Si–OR-terminated silicon quantum dot is typified by an emission centered at 600 nm.[20,30]

Further insights into the nature of the photoluminescence can be obtained by analyzing the time-resolved photoluminescence spectra from the allylamine-capped silicon quantum dots in water. Figure 5 shows the time-resolved photoluminescence decays from an aqueous solution of allylamine-capped silicon quantum dots at two different emission wavelengths. The PL decay measured at 420 nm (Figure 5, curve a) is noticeably shorter than the PL decay measured at 500 nm in curve b. Both PL decays required a three exponential fit with an overall average decay of 4 ns.

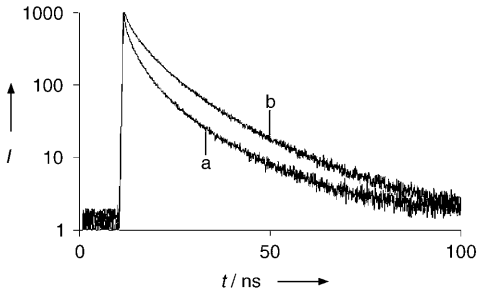

Figure 5. Time-resolved photoluminescence decays of allylamine-capped silicon quantum dots in water measured at emission wavelengths a) 420 nm and b) 500 nm. An excitation wavelength of 380 nm was used.

Indirect band gap materials, such as silicon, generally have slow recombination with PL lifetimes on the order of tens of microseconds to milliseconds, whereas direct band gap materials, such as GaAs and CdSe, have fast recombination with PL lifetimes on the order of 1–10 ns.[31] The PL lifetime measurements obtained here are in good agreement with the experimental findings of the research groups of Korgel [23] and Wilcoxon[20] as well as the theoretical predictions of Zhou et al.[18] The rapid rates of recombination measured here provide strong evidence that the observed emission results from dipole-allowed recombination across the direct band gap transition in silicon quantum dots with a carbon surface termination.

The suitability of allylamine-capped silicon quantum dots as a chromophore for biological imaging is demonstrated in Figure 6, for which an excitation wavelength of 365 nm was used and the emission at 480 nm was monitored. The control image (Figure 6a) shows minimal fluorescence from the HeLa cells relative to the HeLa cells with the incorporated silicon quantum dots (Figure 6b). Thus, the fluorescence observed in the HeLa cells in Figure 6b arises from the emission from silicon quantum dots and not autofluorescence from the cells. The inset in the top left corner of Figure 6b shows the bright blue fluorescence from a vial of allylamine-capped silicon quantum dots in water when excited with UV light. The bright blue fluorescence from the silicon quantum dots is distributed uniformly inside the cytosol of the HeLa cells and this shows the possibility of using these hydrophilic silicon quantum dots as chromophores in biological fluorescence imaging. This result has major implications towards

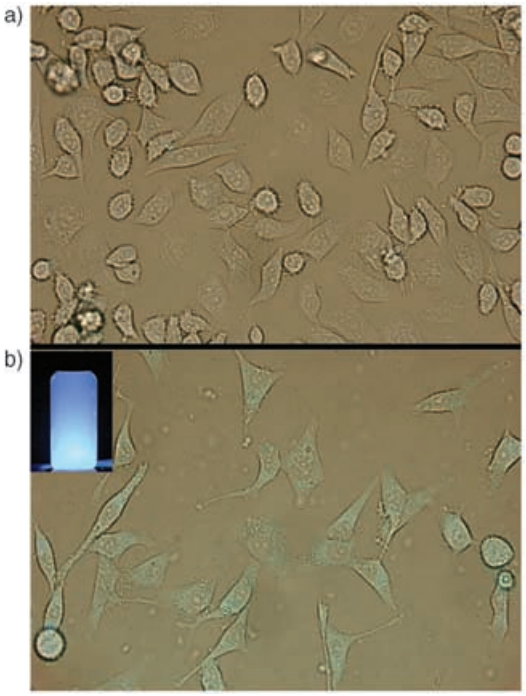

Figure 6. Overlay of the transmission and fluorescence microscope images of a) HeLa cells in the absence of any quantum dots and b) HeLa cells with silicon quantum dots incorporated inside the cytosol. Inset: fluorescence from a vial of allylamine-capped silicon quantum dots in water when excited with a UV lamp.

using colloidal silicon quantum dots effectively in biological fluorescence imaging.

In summary, silicon quantum dots with a narrow size distribution were synthesized using reverse micelles and powerful hydride reducing agents at room temperature and pressure. The surface of the silicon quantum dots was made hydrophilic by modification with allylamine. The silicon quantum dots dispersed in an aqueous environment displayed strong photoluminescence in the blue region of the visible spectrum, with a 10% quantum yield for the photoluminescence. The optical properties of the silicon quantum dots displayed features in both the absorption and emission spectra attributed to the direct band gap transitions in silicon quantum dots with a carbon surface termination. Time-resolved photoluminescence spectroscopy revealed a rapid recombination normally associated with direct band gap materials. The ease of synthesis and optical properties make the silicon quantum dots reported here excellent candidates for biomedical applications, as demonstrated by the imaging of allylamine-capped silicon quantum dots in HeLa cells.

Experimental Section

Synthesis of allylamine-capped silicon quantum dots: Silicon quantum dots were synthesized in reverse micelles by the solution-phase reduction of $SiCl_4$ with 1 M $LiAlH_4$ in THF (Aldrich). The surfactant and solvent combination used to form the micelles were tetraoctylammonium bromide (TOAB, Merck) in toluene. Surface modification of the silicon quantum dots was achieved by treating the surface of the particles with allylamine (Aldrich). All experiments were carried out in an argon atmosphere in a glove box to prevent oxidation of the silicon. Oxygen levels were below 10 ppm at all times.

In a typical experiment, $SiCl_4$ (92 μL, 0.0008 mol) was dissolved in TOAB (1.5 g) and anhydrous toluene (100 mL) by using a homogenizer. Silicon quantum dots were then formed by adding a twofold excess of reducing agent. The mixture was left to react for 3 h and then anhydrous methanol (20 mL) was slowly added to quench any excess reducing agent. At this point it is expected that the surface of the particles were terminated with hydrogen.[20,25] Hydrophilic particles were formed by modifying the surface silicon–hydrogen bonds by reaction with 0.05 M H_2PtCl_6 (40 μL) in isopropanol as the catalyst and allylamine (2 mL). After modification of the surface, the sample was removed from the glove box and purified by removing the surfactant.[32] The solvent was then removed using a rotary evaporator to produce a white powder consisting of mainly TOAB and silicon quantum dots. Distilled water (50 mL) was then added to the flask and resulted in the hydrophilic silicon quantum dots dissolving, but not the TOAB. The TOAB was then removed by successive filtration through a 0.22-μm membrane filter.

Incorporation of silicon quantum dots into HeLa cells: The HeLa cells were cultured in DMEM/F12 supplemented with 10% heat-inactivated fetal bovine serum at 37 °C. The cells were plated at a volume of 1×10^6 cells/well on a 6-well culture plate (Iwaki technoglass, Japan) and were stimulated with a solution of 0.2 nM Si quantum dots. After incubation of the mixtures for 12 h, the cells were washed with a phosphate-buffered saline (PBS) twice to remove the nonspecific binding quantum dots. The cells were then fixed with 1% paraformaldehyde in PBS for 5 min.[33] Fluorescence images of the HeLa cells were acquired with a digital camera D1X (Nikon) on a fluorescent microscope IX-81 (Olympus) using a mirror unit to adjust the excitation wavelength to 365 nm and an oil immersion objective lens. The blue fluorescent light was detected in the cytosol of each cell.

Received: April 11, 2005
Published online: June 23, 2005

Keywords: imaging agents · luminescence · nanostructures · quantum dots · silicon

[1] W. C. Chan, S. Nie, *Science* **1998**, *281*, 2016.
[2] M. Bruchez, M. Moronne, P. Gin, S. Weiss, A. P. Alivisatos, *Science* **1998**, *281*, 2013.
[3] M. Green, *Angew. Chem.* **2004**, *116*, 4221; *Angew. Chem. Int. Ed.* **2004**, *43*, 4129.
[4] A. Wu, H. Liu, J. Liu, K. N. Haley, J. A. Tradway, J. P. Larson, N. Ge, F. Peale, M. P. Bruchez, *Nat. Biotechnol.* **2003**, *21*, 41.
[5] B. Dubertret, P. Skourides, D. J. Norris, V. Noireaux, A. H. Brivanlou, A. Libchaber, *Science* **2002**, *298*, 1759.
[6] D. R. Larson, W. R. Zipfel, R. M. Williams, S. W. Clark, M. P. Bruchez, F. W. Wise, W. W. Webb, *Science* **2003**, *300*, 1434.
[7] L. Bakueva, G. Konstantatos, L. Levina, S. Musikhin, E. H. Sargent, *Appl. Phys. Lett.* **2004**, *84*, 3459.
[8] S. A. McDonald, P. W. Cyr, L. Levina, E. H. Sargent, *Appl. Phys. Lett.* **2004**, *85*, 2089.
[9] S. Coe, W. Woo, M. Bawendi, V. Bulovic, *Nature* **2002**, *420*, 800.
[10] T. Tsutsui, *Nature* **2002**, *420*, 752.
[11] W. U. Huynh, J. J. Dittmer, A. P. Alivisatos, *Science* **2002**, *295*, 2425.
[12] R. A. M. Hikmet, D. V. Talapin, H. Weller, *J. Appl. Phys.* **2003**, *93*, 3509.
[13] B. Sun, E. Marx, N. C. Greenham, *Nano Lett.* **2003**, *3*, 961.
[14] C. B. Murray, D. J. Norris, M. G. Bawendi, *J. Am. Chem. Soc.* **1993**, *115*, 8706.
[15] A. M. Derfus, W. C. W. Chan, S. N. Bhatia, *Nano Lett.* **2004**, *4*, 11.

[16] D. K. Nagesha, M. A. Whitehead, J. L. Coffer, *Adv. Mater.* **2005**, *17*, 921.
[17] L. T. Canham, C. L. Reeves, J. P. Newey, M. R. Houlton, T. I. Cox, J. M. Buriak, M. P. Stewart, *Adv. Mater.* **1999**, *11*, 1505.
[18] Z. Zhou, L. Brus, R. Friesner, *Nano Lett.* **2003**, *3*, 163.
[19] J. D. Holmes, K. J. Ziegler, C. Doty, L. E. Pell, K. P. Johnson, B. A. Korgel, *J. Am. Chem. Soc.* **2001**, *123*, 3748.
[20] J. P. Wilcoxon, P. P. Provencio, G. A. Samara, *Phys. Rev. B* **1999**, *60*, 2704.
[21] R. K. Baldwin, K. A. Pettigrew, E. Ratai, M. P. Augustine, S. M. Kauzlarich, *Chem. Commun.* **2002**, 1822.
[22] J. Zou, R. K. Baldwin, K. A. Pettigrew, S. M. Kauzlarich, *Nano Lett.* **2004**, *4*, 1181.
[23] D. S. English, L. E. Pell, Z. Yu, P. F. Barbara, B. A. Korgel, *Nano Lett.* **2002**, *2*, 681.
[24] J. P. Wilcoxon, G. A. Samara, *Appl. Phys. Lett.* **1999**, *74*, 3164.
[25] R. D. Tilley, J. H. Warner, K. Yamamoto, I. Matsui, H. Fujimori, *Chem. Commun.* **2005**, *14*, 1836.
[26] A. Puzder, A. J. Williamson, J. C. Grossman, G. Galli, *J. Am. Chem. Soc.* **2003**, *125*, 2786.
[27] C. Yang, R. A. Bley, S. M. Kauzlarich, H. W. H. Lee, G. R. Delgado, *J. Am. Chem. Soc.* **1999**, *121*, 5191.
[28] A. T. R. Williams, S. A. Winfield, J. N. Miller, *Analyst* **1983**, *108*, 1067.
[29] S. Hamai, F. Hirayama, *J. Phys. Chem.* **1983**, *87*, 83.
[30] Y. Kanemitsu, T. Futagi, T. Matsumoto, H. Mimura, *Phys. Rev. B* **1994**, *49*, 14732.
[31] J. H. Warner, E. Thomsen, A. R. Watt, N. R. Heckenberg, H. Rubinsztein-Dunlop, *Nanotechnology* **2005**, *16*, 175.
[32] R. D. Tilley, S. Saito, *Langmuir* **2003**, *19*, 5115.
[33] A. Hoshino, K. Fujioka, T. Oku, M. Suga, Y. F. Sasaki, T. Ohta, M. Yasuhara, K. Suzuki, K. Yamamoto, *Nano Lett.* **2004**, *4*, 2163.

